Impurity transport through a strongly interacting bosonic quantum gas

T. H. Johnson,[1,*] S. R. Clark,[2,1,3] M. Bruderer,[4] and D. Jaksch[1,2,3]

[1]*Clarendon Laboratory, University of Oxford, Parks Road, Oxford OX1 3PU, United Kingdom*

[2]*Centre for Quantum Technologies, National University of Singapore, 3 Science Drive 2, Singapore 117543, Singapore*

[3]*Keble College, University of Oxford, Parks Road, Oxford OX1 3PG, United Kingdom*

[4]*Fachbereich Physik, Universität Konstanz, D-78457 Konstanz, Germany*

(Received 13 June 2011; published 10 August 2011)

Using near-exact numerical simulations, we study the propagation of an impurity through a one-dimensional Bose lattice gas for varying bosonic interaction strengths and filling factors at zero temperature. The impurity is coupled to the Bose gas and confined to a separate tilted lattice. The precise nature of the transport of the impurity is specific to the excitation spectrum of the Bose gas, which allows one to measure properties of the Bose gas nondestructively, in principle, by observing the impurity; here we focus on the spatial and momentum distributions of the impurity as well as its reduced density matrix. For instance, we show it is possible to determine whether the Bose gas is commensurately filled as well as the bandwidth and gap in its excitation spectrum. Moreover, we show that the impurity acts as a witness to the crossover of its environment from the weakly to the strongly interacting regime, i.e., from a superfluid to a Mott insulator or Tonks-Girardeau lattice gas, and the effects on the impurity in both of these strongly interacting regimes are clearly distinguishable. Finally, we find that the spatial coherence of the impurity is related to its propagation through the Bose gas.

DOI: 10.1103/PhysRevA.84.023617 PACS number(s): 67.85.−d, 05.60.Gg, 47.60.−i, 72.10.−d

I. INTRODUCTION

The transport of an impurity through a Bose gas has received much attention due to both its inherent appeal as an example of nonequilibrium quantum dynamics and its importance in mimicking the transport of an electron in a conductor [1]. The advantage of a cold atom and optical lattice setup is its ability to realize idealized Hamiltonians and fine-tune interactions over large parameter regimes, often beyond those found in condensed matter systems [2]. In this vein, we extend the large body of theoretical work on the transport of an impurity (partly subject to static forcing) through a superfluid [3–9] by considering strongly interacting bosons in one dimension up to the Mott insulator and Tonks-Girardeau limits, whereupon the bosons exhibit fermionic characteristics [10]. Recently, impurity transport in this context has received interest due to its successful realization by two experiments, one using a species specific dipole potential [11] and another using gravity to provide a static force for the impurities [12,13]. In this paper, we look at how an impurity subjected to a one-dimensional tilted optical lattice potential moves through a bosonic lattice gas in diverse regimes. We simulate the system nonperturbatively and near-exactly at zero temperature using the matrix product based time-evolution block decimation (TEBD) algorithm [14,15].

This work also relates to progress made in probing cold atoms in optical lattices. For example, the excitation properties of a Bose gas in an optical lattice can be analyzed using Bragg spectroscopy via two photon scattering [16] and lattice depth modulation [17,18]—the experiment in [17] having been later successfully simulated in [19,20]. Studying the transport of a Bose gas after imparting a momentum on it using a magnetic field [18] or tilting the lattice [21] has allowed experimentalists to successfully reveal signatures of phase transitions or determine excitation spectra, respectively. A Bose-Einstein condensate has been used as a source of matter waves to infer the spatial properties of atoms in a Mott insulator through Bragg diffraction [22]. Recently, an impurity has been used in experiments as a coherent probe for large quantum systems in order to extract impurity-boson collision parameters [23] and interaction strengths [24].

We here combine and extend these two ideas of probing a system using impurities and transport; we discuss how the motion of an impurity depends on its environment and then, using our simulations, we show what information can be revealed about the environment nondestructively by observing the impurity. As our example, we consider the environment to be a Bose lattice gas and demonstrate that by analyzing the transport of the impurity one can determine the bandwidth and the gap in the excitation spectrum of the Bose gas. In the case of a commensurately filled Bose gas, the impurity propagation provides a clear signature of the superfluid to Mott insulator transition in the form of a sharp quench of the expected current. The strong dependence on the filling allows one to determine nondestructively whether the bosons have been prepared in a commensurately filled state, as desired in some applications of quantum information processing.

The structure of this article is as follows. In Sec. II, we develop the theoretical framework underlying the dynamics of impurities in a tilted lattice, first decoupled and then coupled via interactions to an environment. Subsequently, we specialize to the case of an environment constituting a Bose lattice gas. In Sec. III, we simulate the propagation of the impurity. Specifically, in Secs. III A and III B, we analyze the displacement of the impurity in an incommensurately and commensurately filled Bose gas, respectively, and show that deviations from the basic Esaki-Tsu dependence on tilt clearly reveal information about the gas. In Sec. III C, we show how the interaction of the impurity with the Bose gas affects the

*t.johnson1@physics.ox.ac.uk

momentum distribution of the impurity. Then, in Sec. III D, we discuss the decoherence of the impurity. We make our conclusions in Sec. IV and leave a brief review of the TEBD algorithm to the Appendix.

II. THEORETICAL FRAMEWORK

A. Impurities in a tilted lattice

In our system, we have one or a few impurities confined to a tilted optical lattice, which allows them to move along one spatial dimension only, depicted in Fig. 1(a). Such an optical lattice can be created for the impurities by subjecting them to both an optical lattice and a static forcing, e.g., gravity [12], or by chirping the frequency difference between the counterpropagating lasers making up the standing wave of an optical lattice along the direction of motion [25]. For sufficiently deep lattices and low temperatures, solely the lowest Bloch band is occupied and only tunneling between nearest-neighbor sites must be considered. The Hamiltonian of the impurities is of the form

$$\hat{H}_a = -J_a \sum_{\langle i,j \rangle} \hat{a}_i^\dagger \hat{a}_j + \Delta \sum_i i \hat{a}_i^\dagger \hat{a}_i, \tag{1}$$

where $\langle i,j \rangle$ denotes nearest-neighbor sites i and j, and $\hat{a}_i^\dagger$ ($\hat{a}_i$) is the creation (annihilation) operator for an impurity in a Wannier state [26] localized at site i, separated in energy and distance from its neighbors by the Bloch energy Δ and the lattice constant a. An additional condition for the above Hamiltonian to hold is that the separation of the Bloch bands must be much greater than the Bloch energy. Note that the impurities could be either bosonic or fermionic; we assume them to be sufficiently dilute so that impurity-impurity interactions and their quantum statistics have negligible effects.

Without a further interaction with an environment, it is not possible for an impurity to dissipate energy and therefore alter its expected position. The eigenstates of the Hamiltonian in Eq. (1) are centered at each of the lattice sites i and have energies Δi forming the so-called Wannier-Stark ladder of states. Introducing the width $\Lambda = 2J_a/\Delta$, the creation operator for a Wannier-Stark state is defined by $\hat{d}_i^\dagger = \sum_j \mathcal{J}_{j-i}(\Lambda)\hat{a}_j^\dagger$, where $\mathcal{J}_n(\Lambda)$ is a Bessel function of the first kind of order n. As the states are separated by an energy Δ, a superposition of them oscillates at a frequency $\Delta/\hbar$.

This Wannier-Stark picture is consistent with the solution of the semiclassical equations for an impurity in a lattice described by a wave packet of well-defined quasimomentum (therefore, spatially it must be spread over many lattice sites) [27]. In such a framework, the effect of the tilt is a constant drift of the quasimomentum of each of the impurities at rate $\dot{k} = \Delta/\hbar a$. Together with the semiclassical equation of motion for the group velocity of a wave packet,

$$v(k) = \frac{1}{\hbar}\frac{\partial E}{\partial k}, \tag{2}$$

and the single-particle energy spectrum in a lattice $E(k) = 2J_a(1-\cos ka)$, this results in a group velocity that is sinusoidal in time. Thus an impurity undergoes harmonic motion with frequency $\Delta/\hbar$, but there is no net drift down the lattice. Although originally derived semiclassically, these Bloch oscillations are a purely coherent phenomenon, can be arrived at quantum-mechanically, and are rigorously connected to the Wannier-Stark picture [28]. In Fig. 2(a), we show the coherent Bloch oscillation of an impurity initially located in a Wannier state.

We note that Bloch oscillations in semiconductors are usually obscured by large scattering rates, though they have been observed in superlattices where the Bloch frequencies $\Delta/\hbar$ achievable are much higher due to larger lattice spacings [30]. Bloch oscillations are also observable in analogous optical lattice setups, as we find here, due to the much smaller scattering rates.

B. Impurities coupled to an environment

If the impurities are coupled to an environment, then this introduces a mechanism through which an impurity can dissipate energy and fall down the lattice. Esaki and Tsu [31], using the semiclassical Bloch oscillation picture, derived an expression for the average current in the relaxation-time approximation. The main assumption is that an impurity suffers collisions at some rate $1/\tau$ that resets its momentum distribution to that of thermal equilibrium (we assume zero temperature here). The resulting expression for the average velocity of each of the impurities is then

$$\langle v \rangle = \frac{2aJ_a}{\hbar}\frac{\tau\Delta/\hbar}{(\tau\Delta/\hbar)^2+1}, \tag{3}$$

describing a linear (ohmic) dependence on forcing at small $\tau\Delta/\hbar$ followed by negative differential conductance as $(\tau\Delta/\hbar)^{-1}$ when $\tau\Delta/\hbar \gg 1$. This dependence is plotted in Fig. 2(b). In this semiclassical framework, the negative differential current arises if the time scale of the collisions is considerably larger than the period of Bloch oscillations, in which case the velocity of the impurity is not always in the same direction and averages out between collisions. Negative differential conductance, as with Bloch oscillations, is usually obscured in semiconductors but, due to the much larger values of $\tau\Delta/\hbar$ achievable, it has been observed in optical lattices [32] and superlattices [33].

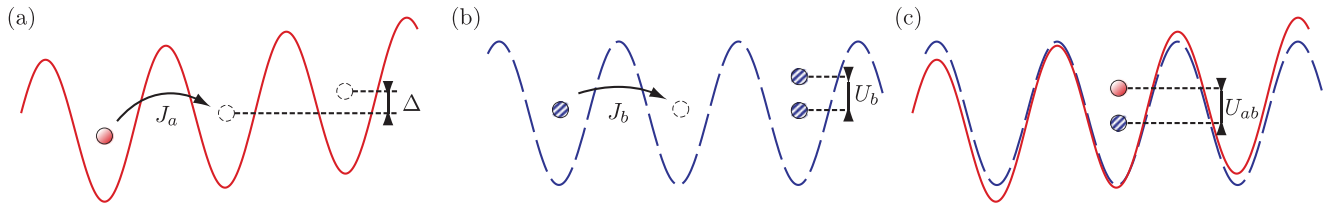

FIG. 1. (Color online) Schematic diagram for the (a) impurity, (b) Bose gas, and (c) interaction Hamiltonians.

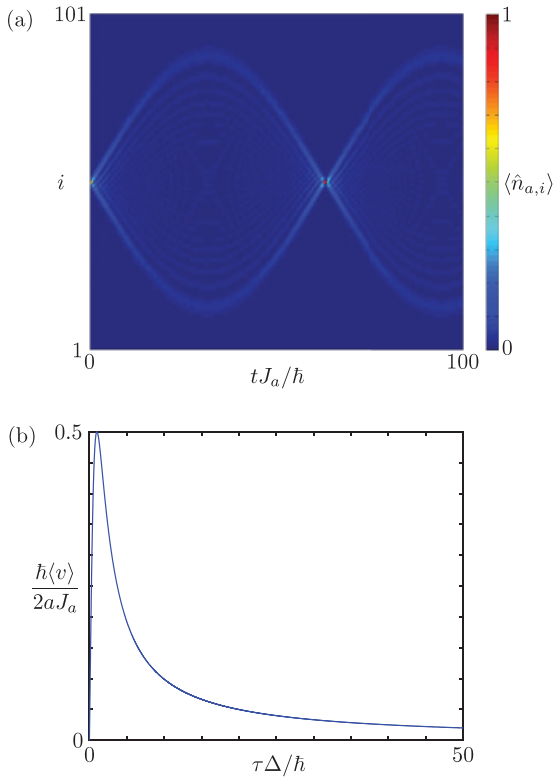

FIG. 2. (Color online) Motion of a single impurity in a tilted lattice with and without a scattering process. (a) The impurity decoupled from any environment will coherently Bloch oscillate at frequency $\Delta/\hbar$, but its expected position will not drift [5,29]. Here we plot the evolution in time t for just over one and a half Bloch oscillations. The impurity is initially localized in a Wannier state at the middle site of the 101-site lattice. We set the tilt to be $\Delta/J_a = 0.1$ and $\langle \hat{n}_{a,i} \rangle$ is the impurity density at lattice site i. (b) Introducing a scattering mechanism under the relaxation-time approximation results in the Esaki-Tsu dependence of drift on tilt in Eq. (3). We plot this dependence here.

Clearly the relaxation-time approximation is not always valid and the actual current will depend on the details of the environment and its interaction with the impurity. However, it has been found that, at least qualitatively, an Esaki-Tsu–like dependence of current on forcing is obeyed in many cases: for density-density interactions between an impurity and a Bose lattice gas at finite [8,34] and infinite temperatures [4,35] (see [36] for a discussion from the perspective of quantum chaos); when an impurity scatters from a set of different fixed impurities with scattering resulting in a Fermi distribution in momentum space [37]; and where an impurity scatters on phonons [38].

Turning this on its head, the precise way in which the current of the impurity deviates from the Esaki-Tsu dependence reveals information about the environment and impurity-environment interaction. For example, the ability to excite optical phonons in the environment at a single frequency results in resonances in the current of an impurity at certain tilts dependent on this frequency [38]. The interaction of impurities with a superfluid in a lattice, which has a divergence in the density of phonon states at the band edge, also causes peaks at forcings related to fractions of the bandwidth [8].

We now consider in which way properties of the environment manifest themselves in the current of the impurities, approaching the problem using both the semiclassical and Wannier-Stark pictures.

1. Scattering in momentum space

First, we use the semiclassical approach where the distribution of impurities in quasimomentum space $g(k)$ obeys the Boltzmann equation [27],

$$\frac{dg(k)}{dk} = \frac{\hbar a}{\Delta} \int dq [W(q,k)g(q) - W(k,q)g(k)], \qquad (4)$$

which is valid for homogeneous systems of impurities in the steady state and where $W(q,k)$ is the rate of incoherent scattering between quasimomenta q and k. The average velocity of each impurity is then the expected value of the group velocity of wave packets distributed according to $g(k)$,

$$\langle v \rangle = \int dk\, g(k) v(k), \qquad (5)$$

where the group velocity for a particular quasimomentum is defined in Eq. (2). Several choices of scattering rates lead to the motion of the impurity exhibiting exactly or approximately an Esaki-Tsu dependence [31,35].

For small enough tilts, the quasimomentum will be a very slowly changing quantity and hence, for weak interactions with the environment, we may approximate the incoherent scattering rates using Fermi's golden rule as

$$W(q,k) = \frac{2\pi}{\hbar} \sum_{n_b} |\langle k\, |\langle n_b\, |\hat{H}_{ab}|\, q\rangle |\, 0_b\rangle|^2 \times \delta(E_{n_b} - E_{0_b} - 2J_a[\cos qa - \cos ka]).$$

Here we have assumed the environment to be sufficiently large and cold so that before scattering we may take it to be in the ground state $|\, 0_b\rangle$ of energy E_{0_b}. The result of the interaction of the impurity with the environment, for which the Hamiltonian is given by $\hat{H}_{ab}$, is to scatter the environment to some excited state $|\, n_b\rangle$ with energy E_{n_b}.

Particularly important for our system is the case of impurities coupled to a many-body environment, here the Bose gas, via a density-density interaction. For low energies, the interaction takes the explicit form

$$\hat{H}_{ab} = U_{ab} \sum_i \hat{a}_i^\dagger \hat{a}_i \hat{b}_i^\dagger \hat{b}_i, \qquad (6)$$

where U_{ab} is its characteristic energy and $\hat{b}_i^\dagger$ ($\hat{b}_i$) is the creation (annihilation) operator for a particle in the environment at lattice site i. The corresponding quasimomentum scattering rates are given by [39]

$$W(q,k) = \frac{2\pi U_{ab}^2}{\hbar L} S(q-k, -2J_a[\cos qa - \cos ka]), \qquad (7)$$

where L is the length of the system, $S(q,\omega)$ is the zero-temperature dynamic structure factor of the environment,

$$S(q,\omega) = \textstyle\sum_{n_b} |\langle n_b\, |\hat{\rho}_q|\, 0_b\rangle|^2 \delta(E_{n_b} - E_{0_b} - \hbar\omega),$$

and $\hat{\rho}_q$ is the Fourier transform of the particle density of the environment. Hence the impurity current and, more directly,

the momentum distribution at small tilts are governed by the dynamic structure factor of the environment.

2. *Transitions between Wannier-Stark states*

At larger lattice tilts, it is convenient to work in the basis of Wannier-Stark states and to consider the incoherent transitions between these. The dynamics of the impurities is described by the master equation

$$\frac{dP_i(t)}{dt} = \sum_{j\neq i}[W_{ji}P_j(t) - W_{ij}P_i(t)],$$

with the incoherent hopping rates W_{ij}. The probability P_i that the impurity occupies Wannier-Stark states at site i is normalized to $\sum_i P_i(t) = 1$. The corresponding average velocity then reads

$$\langle v\rangle = \sum_i ai\frac{dP_i(t)}{dt}.$$

Note that in an infinite homogeneous system the average velocity would be $\langle v\rangle = \sum_j a(j-i)W_{ij}$. Again, for weak coupling to the environment the transition rates W_{ij} between different Wannier-Stark states are given by Fermi's golden rule as

$$W_{ij} = \frac{2\pi}{\hbar}\sum_{n_b}|\langle j|\langle n_b|\hat{H}_{ab}|i\rangle|0_b\rangle|^2 \times \delta(E_{n_b} - E_{0_b} + [i-j]\Delta). \quad (8)$$

In this picture, negative differential current arises due to the increasing localization of the Wannier-Stark states: as Δ increases, the width of the Wannier-Stark states decreases as $1/\Delta$, resulting in a suppression of their overlaps and thus the motion of the impurity.

Inserting the interaction Hamiltonian in Eq. (6) into Eq. (8), we arrive at the environment correlation function,

$$W_{ij} = \frac{2\pi U_{ab}^2}{\hbar}\sum_{n_b}\left|\langle n_b|\sum_\ell \mathcal{J}_{\ell-j}(\Lambda)\mathcal{J}_{\ell-i}(\Lambda)\hat{b}_\ell^\dagger\hat{b}_\ell|0_b\rangle\right|^2 \times \delta(E_{n_b} - E_{0_b} + [i-j]\Delta), \quad (9)$$

which determines the current at larger tilts. From this, we immediately see two effects that we expect to be visible in the impurity current. First, consider the case where the environment has a gap G in its excitation spectrum such that $E_{n_b} - E_{0_b} \geqslant G$. This means that the delta function in Eq. (9) will be zero unless $\Delta \geqslant G/(j-i)$ and hence the contributions to the current due to hopping between Wannier-Stark states shifted by ℓ sites will only be made at tilts above $\Delta = G/\ell$. Second, if the excitation spectrum of the environment has a finite bandwidth such that there are no states above an energy B, i.e., $E_{n_b} - E_{0_b} \leqslant B$, then we expect ℓ-site contributions to the current to be suppressed at tilts above $\Delta = B/\ell$. Hence the deviation of the dissipation process from the relaxation-time approximation results in the dependence of the impurity current on Δ exhibiting sharp features that clearly reveal information about the environment; we can infer these environmental properties by observing the impurities.

C. Properties of the Bose gas environment

Our specific environment consists of a Bose gas trapped in a horizontal (nontilted) optical lattice in which the bosons are confined to move in the same single dimension as the impurities. As for the impurities, we consider temperatures to be low enough such that only the lowest Bloch band need be considered. In such a case, the bosons are described by the Bose-Hubbard model [40],

$$\hat{H}_b = -J_b\sum_{\langle i,j\rangle}\hat{b}_i^\dagger\hat{b}_j + \frac{U_b}{2}\sum_i\hat{b}_i^\dagger\hat{b}_i^\dagger\hat{b}_i\hat{b}_i,$$

where the operator $\hat{b}_i^\dagger$ ($\hat{b}_i$) creates (annihilates) a boson in a Wannier state localized at site i and the lattice parameter a is the same as that for the impurities. J_b and U_b are parameters that determine the hopping between neighboring sites and the on-site interaction, respectively, and can be tuned experimentally by adjusting the laser parameters or using Feshbach resonances [2,40].

Let us briefly review some properties of the Bose gas, which we will use to interpret our findings. In the superfluid regime ($U_b/J_b \ll 1$), the Bose gas supports excitations in the form of Bogoliubov phonons, whose excitation spectrum is given by [41]

$$\hbar\omega_k = \sqrt{\varepsilon_k(\varepsilon_k + 2U_b n_b)}, \quad (10a)$$

$$\varepsilon_k = 2J_b(1-\cos ka), \quad (10b)$$

where n_b is the ratio of bosons to lattice sites. From this, we find that the density of states $(\hbar\partial\omega_k/\partial k)^{-1}$ diverges at the upper edge of the band with bandwidth $B = 4J_b\sqrt{1+U_b n_b/2J_b}$. In the opposite limit $U_b/J_b \to \infty$, the bosons map to the same number of noninteracting identical fermions with energy spectrum ε_k. Hence, in this regime, the Bose gas supports particle-hole excitations for $n_b < 1$ within the single band of bandwidth $B = 4J_b$.

For the commensurately filled case of $n_b = 1$, an increasing interaction strength U_b/J_b takes the gas through a continuous superfluid to Mott insulator transition, which occurs at $U_b/J_b = 3.37$ [42,43] in the thermodynamic limit. A principal signature of this transition is the appearance of a gapped excitation spectrum suppressing the low-energy response. Deep in the Mott insulator regime ($U_b/J_b \gg 1$), the gap in the excitation spectrum is $G \simeq U_b$.

D. Detailed model and measuring procedure

To summarize, the model for our system is given by the impurity Hamiltonian $\hat{H}_a$, the Bose-Hubbard model $\hat{H}_b$, and the density-density interaction $\hat{H}_{ab}$, as shown schematically in Fig. 1. More precisely, we consider an M-site system with box boundary conditions or a suitably flat bottomed potential (see [44] for an example of a box trap realized in an experiment). As argued in [8], we expect our system to share its bulk behavior with the experimentally important case of an additional harmonic trap, provided that the trap is sufficiently shallow. A realization of the model may also draw on recent experimental successes in trapping atoms in species-specific optical lattices [11,45,46].

The system is the same as that considered in [4], where for low tilts $\Delta/J_b \ll 1$ they used that the relevant correlation functions of the Bose gas decay quickly enough to allow the dynamics of the impurity to be described by a Markovian master equation. For the same system, Ref. [47] uses the chaotic system approach along with Kubo's formalism to derive the current in the ohmic region $\Delta\tau/\hbar \ll 1$. We also considered this system in [8] focusing on a superfluid environment ($U_b/J_b \ll 1$), in which the impurity and Bose gas together mimicked the electron-phonon interaction. However, the control and flexibility of an optical lattice setup allows for the creation of a strongly interacting Bose gas ($U_b/J_b \gg 1$), the regime we explore in this paper.

To measure the impurity current, we propose the following procedure. The N bosons are cooled to their ground state with the impurities fixed in highly localized states at their initial locations (for example, using a tight optical trap). The system reaches equilibrium and the presence of the impurities inevitably leads to density variations in the initial state of the bosons as compared to the ground state of the Bose-Hubbard Hamiltonian. At time $t = 0$, the impurities are released, their lattice is tilted, and the system is left to evolve. Later, a time-of-flight measurement [2] or *in situ* image [48,49] is taken.[1] Note that alternative preparations of the initial state we considered, e.g., preparing the bosons in equilibrium without the impurities and then adding the impurities at $t = 0$, produced the same qualitative results despite this being a more energetic initial state.

For our numerical simulations, we consider the complete two-species system governed by the Hamiltonian $\hat{H}_a + \hat{H}_b + \hat{H}_{ab}$. The simulations of the full many-body quantum dynamics at zero temperature are performed using the TEBD algorithm. This is a matrix product based method extending the powerful density matrix renormalization group to real time evolution. We present an overview of the method in the Appendix along with the algorithm parameters used.

We consider a single impurity initially localized in a Wannier state at the center of the lattice. We evolve the system up to $t_{\rm sim} \approx M\hbar/4J_b$, the time it approximately takes the disturbances in the bath caused by the impurity to reach the boundaries of the system, thus minimizing finite-size effects. This time limit is determined by the maximum group velocity v_g of the bosons in the band, which can be derived in both the superfluid $U_b/J_b \to 0$ and strongly interacting $U_b/J_b \to \infty$ limits by differentiating $\hbar\omega_k$ and ε_k [Eqs. (10)], respectively, with respect to k. The time taken for disturbances in the Bose gas to travel a distance $Ma/2$ to the edge of the system is then $Ma/2v_g$, from which the previous expression for $t_{\rm sim}$ follows. We choose to hold the interaction between the impurity and the bosons constant at $U_{ab}/J_b = 0.5$ and the impurity hopping at $J_a/J_b = 0.6$. These values are chosen to reflect the behavior we observed over a wide range. Notably, they are outside the perturbative regime used in Sec. II, yet still lead to the predicted effects.

[1]Over multiple realizations, this allows the calculation of the elements of the reduced single-particle density matrix in the Wannier basis $\langle \hat{a}_i^\dagger \hat{a}_j \rangle$ or its diagonal, the density distribution.

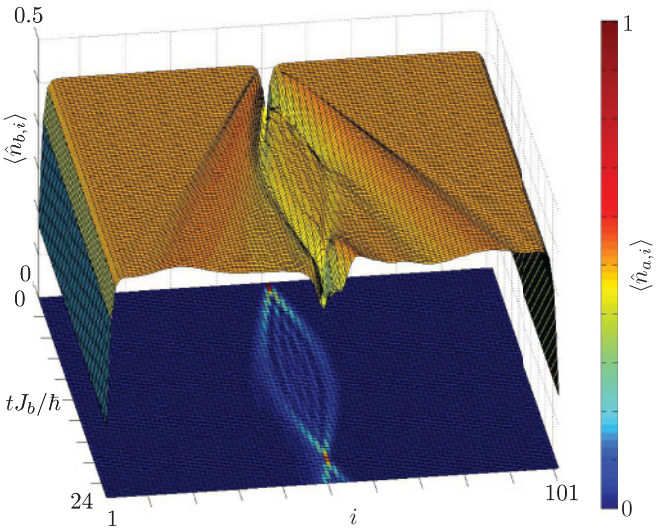

FIG. 3. (Color online) Transport of an impurity through a bosonic bath. An example of the evolution of the impurity and boson densities for the case $\Delta/J_b = 0.3$, $U_b/J_b = 2$, $M = 101$, and $N = 50$. The color map in the xy plane shows the expected impurity density at each lattice site $\langle \hat{n}_{a,i} \rangle$, and similarly for the surface plot and boson density $\langle \hat{n}_{b,i} \rangle$.

III. SIMULATIONS OF IMPURITY PROPAGATION

As a demonstration of the system and numerical method, we show the evolution of both the impurity and bosons in Fig. 3 for an intermediate boson-boson interaction strength $U_b/J_b = 2$. The impurity undergoes Bloch oscillations as it would if the bosons were not present—see Fig. 2(a)—however, the nonzero impurity-boson interactions cause the impurity to dissipate energy into the Bose gas and drift down the lattice. The same interactions also create density fluctuations in the Bose gas, which spread out and reach the system boundary near the end of the simulation.

Examining the system for a range of tilts Δ allows us to find the dependence of impurity displacement $\langle \hat{x}_a \rangle = \sum_i a(i_0 - i)\langle \hat{n}_{b,i} \rangle$ on Δ, where i_0 is the site at which the impurity was initially localized. Using this, we can calculate the average impurity velocity $\langle v \rangle = \langle \hat{x}_a \rangle / t_{\rm sim}$. From detailed examination of our simulations, we find that the displacement does not increase just linearly in time but oscillates slightly at the frequency of the Bloch oscillations (as would be observed in an experiment). For all but the lowest tilts, the durations of evolutions considered is sufficient that by $t_{\rm sim}$ the displacement has averaged over enough Bloch oscillations that $\langle v \rangle$ gives a good representation of the long-time average drift.

A. Superfluid and Tonks-Girardeau regimes

Our starting point is the propagation of the impurity through a Bose gas in the superfluid regime with incommensurate filling. A typical dependence of the displacement of the impurity $\langle \hat{x}_a \rangle$ on the lattice tilt Δ is given by the red circles in Fig. 4(a). This dependence has the characteristic features of the Esaki-Tsu result, shown in Fig. 2(b), namely an ohmic region followed by negative differential conductance [4,8,31].

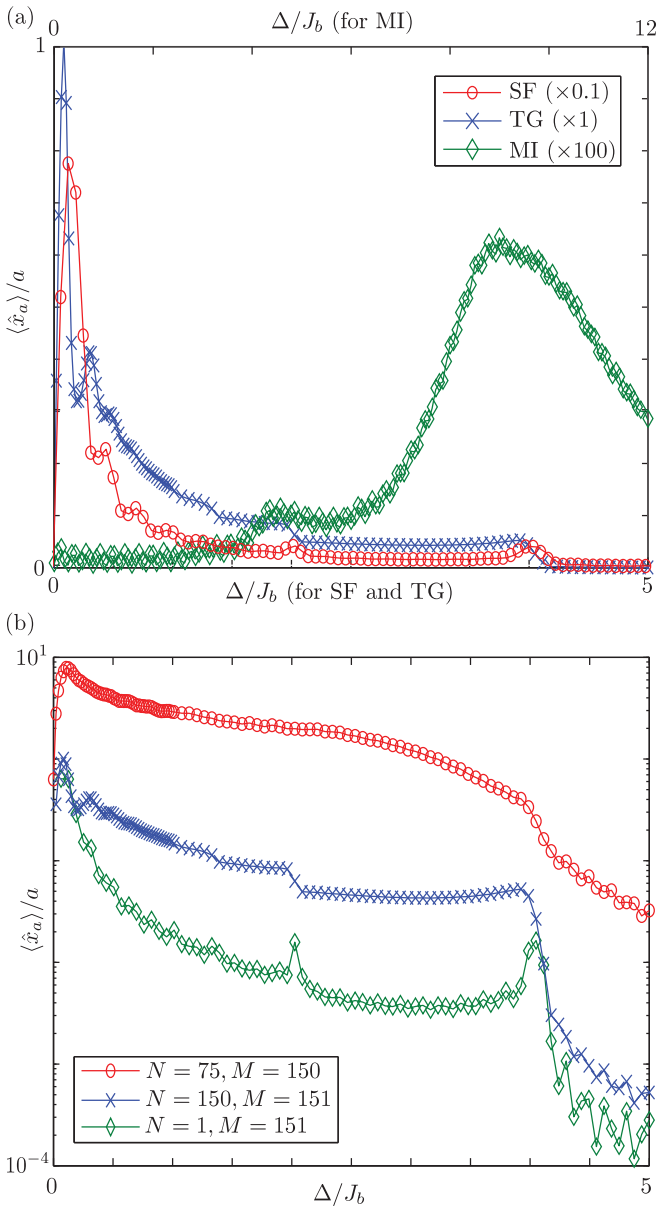

FIG. 4. (Color online) Determining the bandwidth and gap from the dependence of displacement on tilt. (a) The dependence of the displacement of the impurity $\langle\hat{x}_a\rangle$ at t_{sim} as a function of tilt Δ for three regimes of the Bose gas: the superfluid regime $U_b/J_b = 0.1$ with $N = 50$, $M = 101$ (SF: displacement scaled down by a factor of 0.1); the Tonks-Girardeau limit $U_b/J_b \to \infty$ with $N = 150, M = 151$ (TG); and the Mott insulating regime $U_b/J_b = 10$ with $N = M = 101$ (MI: displacement scaled up by a factor of 100). (b) The same quantity is plotted for several bosonic systems in the Tonks-Girardeau limit, demonstrating that the qualitative shape and the positions of the bandwidth suppressions are independent of the filling (so long as it is incommensurate) of the Bose gas.

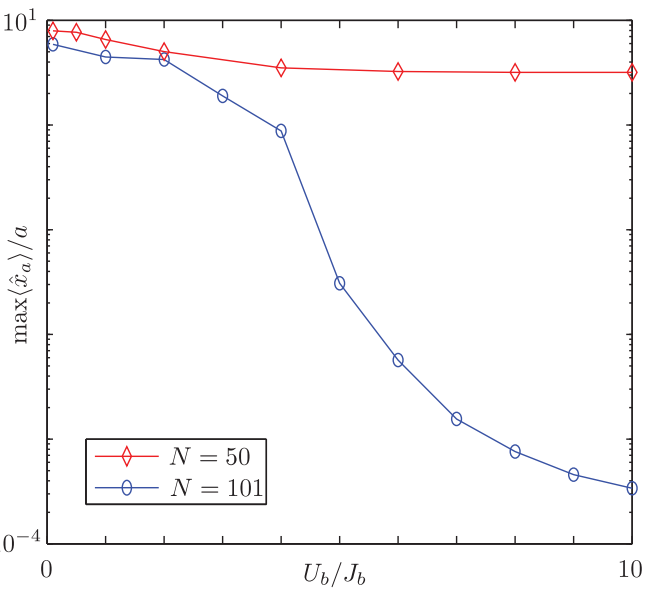

FIG. 5. (Color online) Suppression of average drift in the strongly interacting regimes. Here we show the peak displacement (maximized over all tilts) as a function of interaction strength U_b/J_b for commensurate and incommensurate fillings of a 101-site bosonic lattice.

However, a phenomenon that is specific to the case where the bosons feel a lattice is the occurrence of resonances in the vicinity of the lattice tilts $\Delta = 4J_b/\ell$ for integer $\ell \geqslant 1$. As shown in [8], we expect resonances at tilts $\Delta = (4J_b/\ell)\sqrt{1 + U_b n_b/2J_b}$ corresponding to a divergence in the density of phonon states at the upper band edge. Moreover, the suppression of the propagation of the impurity for $\Delta \gtrsim 4J_b/\ell$ reflects the sudden inability of the impurity to move ℓ sites down the lattice by dissipating the energy $\ell\Delta$ into the Bose gas through a single phonon process. Hence the superfluid Bose gas is a prime example of how the value of the bandwidth of its excitation spectrum B manifests itself in the dependence of the current of the impurity. Note that the small fluctuations in the dependence of drift on tilt at small tilts in Fig. 4(a) are a result of the finite time of our simulations and would be smoothed out by considering longer times. The same would be true in an experimental realization.

One expects to see the bandwidth dependent features even with strong boson-boson interactions; the reasoning used to predict current dropoffs after $\Delta = B/\ell$ in Sec. II assumes the bosonic system is susceptible to low-energy excitations, which is the case for incommensurately filled systems of any interaction strength [41]. Indeed, we have simulated $M = 25$ site systems over a range of boson-boson interaction strengths U_b/J_b (not shown here) and found no qualitative change in the behavior of the motion. However, as shown in Fig. 5, the average displacement of the impurity decreases with increasing interaction strength.

In the extreme case of infinitely strong interactions $U_b/J_b \to \infty$, i.e., in the Tonks-Girardeau limit, the situation simplifies considerably. The bosons map to identical non-interacting fermions with bandwidth $B = 4J_b$, and so the creation of particle holes at the Fermi surface provides low-energy excitations. Accordingly, we expect a large impurity displacement at low lattice tilts and sharp drops in propagation for tilts above integer divisions of the bandwidth $4J_b/\ell$, in agreement with Fig. 4(a).

We find the same behavior in the Tonks-Girardeau limit for many different bosonic filling factors, as shown in Fig. 4(b). The half-filled bosonic system gives rise to a peak impurity

current that is an order of magnitude above that for the cases where the bosonic lattice is filled by a single or $M-1$ bosons. This can be attributed to there being a greater number of excitations available in the half-filled bosonic system; using the fermionic mapping, we find there are approximately $M^2/4$ single quasiparticle excitations available in the half-filled case as compared to $M-1$, when there is only one boson or $M-1$ present. This reasoning suggests that the peak displacement may be used as a measure of the filling of the bosonic system.

B. Superfluid to Mott insulator transition

We now turn to the case of a commensurately filled Bose gas and the continuous superfluid to Mott insulator transition. Since motion of the impurity through the superfluid at low lattice tilts is a result of the ability of the bosons to accept low-energy excitations, we expect propagation to be highly suppressed in the Mott insulator phase, which has a gap in the excitation spectrum of $G \simeq U_b$.

The effect of this signature on the propagation can be seen in Fig. 4(a), where the displacement has a peak at $\Delta \approx U_b$. There is also a second peak at $\Delta \approx U_b/2$ resulting from second-order processes involving two lattice-site jumps, similar to what is seen using Bragg spectroscopy in [19] and tilting the bosonic lattice in [21]. As in those cases, the nonzero J_b results in a broadening of the peaks. This behavior confirms the predictions in Sec. II for the transport of an impurity in a gapped environment. This drastic change from the behavior predicted by Esaki and Tsu also tells us that the relaxation-time approximation is not at all valid for the interaction of an impurity with a Mott insulator.

For small tilts, the motion of the impurity caused by low-frequency excitations is completely suppressed; at large enough U_b/J_b, the ground state is well approximated by a unit-filled Fock state. In such a regime, the impurity Bloch oscillates as it has no means of dissipating energy into the Bose gas; hence there is no net current across the lattice. As a result, we get a startlingly clear signature of the superfluid to Mott insulator transition in our dynamics in the form of a quench of more than four orders of magnitude in the propagation of the impurity. This is shown in Fig. 5.

As well as the ability to probe the superfluid to Mott insulator transition using the impurity, this quench provides a nondestructive way of establishing whether the bosonic system is commensurately filled or not. If our system is strongly interacting $U_b/J_b \gtrsim 4$, there are several orders of magnitude separating the currents for an impurity in the commensurate and incommensurate cases, shown in Fig. 5. Many implementations of quantum information processing involve creating a commensurately filled system. Using an impurity as a probe is one way in which this commensurability could be checked nondestructively.

C. Quasimomentum distribution of the impurity

Alternatively, one can gain information about the impurity by looking at its quasimomentum distribution, which is directly accessible in time-of-flight experiments. With the impurity prepared in a Wannier state, each quasimomentum state is equally occupied. However, we expect interactions with the Bose gas to alter this momentum distribution, resulting in the drift seen in Sec. III. The current $\langle v \rangle$ can be calculated from the distribution in the semiclassical picture using Eq. (5).

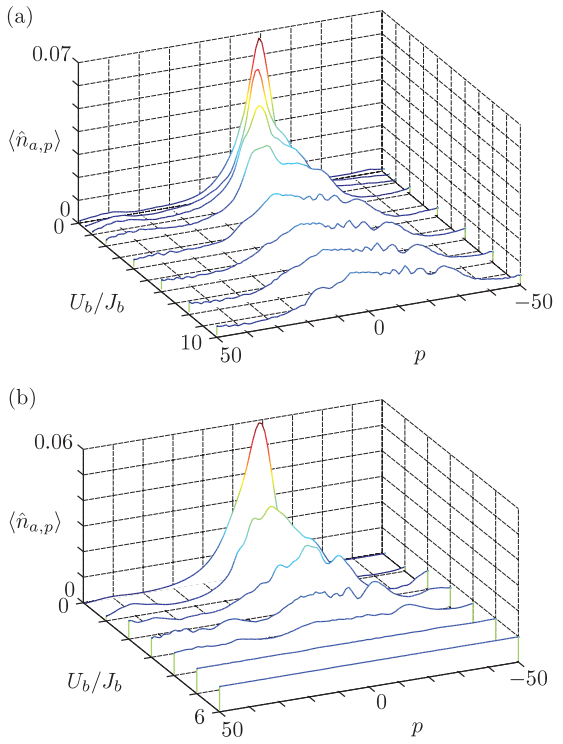

FIG. 6. (Color online) Quasimomentum distribution of the impurity after traveling through the Bose gas. Here $\Delta/J_b = 0.063, M = 101$ and $\hat{n}_{a,p}$ is the number operator for an impurity quasimomentum of $2\pi p/aM$. (a) The momentum distribution of the impurity at t_{sim} for a range of interaction strengths U_b/J_b and incommensurate filling $N = 50$. (b) The same as (a), but for commensurate filling $N = 101$.

As can be seen in Figs. 6(a) and 6(b), the result of interactions with the Bose gas is the enhancement of the distribution near the center of the Brillouin zone. Moreover, the interaction gives rise to an asymmetry with the distribution skewed toward negative quasimomentum, necessary for the impurity to have a current.

Our simulations show that a well-defined quasimomentum emerges in the superfluid regime by the time t_{sim}, supporting the accuracy of the semiclassical approximation. However, for stronger bosonic interaction strengths, the scattering results in a wide distribution with a negative quasimomentum shoulder. By $U_b/J_b \approx 10$, the distribution already approximates its $U_b/J_b \to \infty$ value. In the case of the Mott insulating regime in Fig. 6(b), it is unchanged from its initially flat distribution. Once again, the momentum distribution of the impurity provides a signature of the transition (crossover) between the superfluid and Mott insulator (Tonks-Girardeau) regimes.

The difference in steady-state quasimomentum distribution is related to the structure factor of the Bose gas, cf. Eqs. (4) and (7), but a quantitative comparison with our simulations is difficult since, in general, they do not reach the steady state.

Since this limitation is due to the finite time of our simulations, it would also restrict an experimental realization.

D. Reduced density matrix of the impurity

So far we have focused on the evolution of the spatial and quasimomentum distributions of the impurity; however, more information is contained in its reduced density matrix $\hat{\rho}_a$. First, evaluating the elements of the density matrix in the Wannier basis $\langle \hat{a}_i^\dagger \hat{a}_j \rangle$ may tell us more about the effect of boson-impurity interactions on the impurity. Another quantity that can be calculated from the reduced density matrix is the purity $\mathrm{Tr}(\hat{\rho}_a^2)$, which takes the maximal value 1 if $\hat{\rho}_a$ describes a pure state and decreases for increasingly mixed states. The initial state of the total system is a product of pure states for the impurity and bosons, and since we consider coherent evolution it remains pure. However, through interactions of the impurity with the Bose gas, the two subsystems are entangled, resulting in a loss of purity of the impurity. Our bosonic environment is sufficiently large that for most parameter values revivals are not observed and so we use purity to quantify the decoherence of the impurity.

To demonstrate the behavior of the density matrix $\hat{\rho}_a$ for a $M = 101$ site system, we have plotted in Figs. 7(a) and 7(b) the absolute values of its Wannier basis elements at t_{sim} for both intermediate and weak bosonic interaction strengths, respectively (the elements of $\hat{\rho}_a$ in the quasimomentum basis were calculated for $M = 7$ sites in [47]). In Fig. 7(a), we observe a symmetric coherent interference pattern in the off-diagonal elements as the impurity undergoes Bloch oscillations. Additionally, density-density interactions with the bosons result in a slight decay of the off-diagonal coherences and an asymmetric distribution along the diagonal with a higher occupancy of the lower-energy lattice sites. This decoherence is much more pronounced for a superfluid environment, as shown in Fig. 7(b), and the resulting density matrix is nearly diagonal.

To make this relationship between the decoherence of the impurity and the internal interaction strength of the environment clearer, Fig. 7(c) shows the purity of the reduced density matrix of the impurity as a function of both tilt Δ and interaction strength U_b/J_b. As can be seen in the figure, the coherence of the impurity is a clear signature of the crossover between the superfluid and Tonks-Girardeau regimes. Moreover, the values of U_b/J_b at which the most significant changes occur is around the same values where the transition occurs in a commensurate Bose gas. We also calculated the entanglement entropy between the impurity and Bose gas (not shown here), which showed very similar behavior to purity. If the Bose gas is commensurately filled, the transition between weak and strong interaction strengths makes an even clearer impact on the purity as deep in the Mott insulator phase the impurity does not become at all entangled with the Bose gas.

Finally, comparing Figs. 7(c) and 3(d), we find that the regimes of high transport coincide with those of the smallest purity; the very same scattering processes that lead to the propagation of the impurity along the lattice also cause its decoherence. This relationship between decoherence and transport of the impurity was also found in the case where the impurity undergoes spontaneous emission [50].

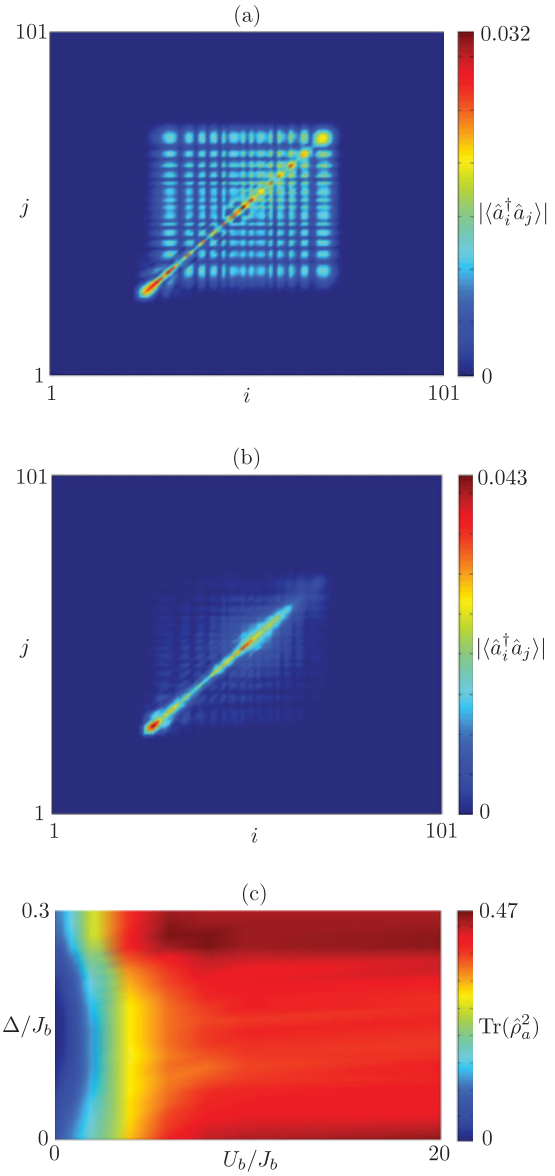

FIG. 7. (Color online) Decoherence of an impurity traveling through an incommensurately filled system $N = 50, M = 101$. (a) Absolute values of the elements of the reduced density matrix for the impurity $|\langle \hat{a}_i^\dagger \hat{a}_j \rangle|$ with $U_b/J_b = 2$ and $\Delta/J_b = 0.1$, calculated at t_{sim}. (b) The same as (a), but for $U_b/J_b = 0.1$. (c) Also at t_{sim} we have plotted the purity of the density matrix $\mathrm{Tr}(\hat{\rho}_a^2)$ as a function of tilt and interaction strength.

IV. CONCLUSIONS

We performed fully quantum many-body simulations of large (100 or more sites) two-species systems using the TEBD algorithm, simulating the one-dimensional motion of an impurity confined to a tilted optical lattice through a Bose lattice gas. We discussed the Esaki-Tsu dependence of the current of the impurity on tilt and provided evidence that this shape is qualitatively obeyed by an impurity traveling through an incommensurately filled bosonic system of any interaction

strength including the Tonks-Girardeau limit. Contrasting this, a very different dependence was found in the Mott insulating regime.

We discussed how deviations to the Esaki-Tsu shape depend on properties of the Bose gas. Information about the gas can then be extracted without needing to measure the bosons themselves, i.e., nondestructively. In particular, we discussed how the impurity could be used to probe the commensurateness of the system, and obtain the gap and bandwidth of its excitation spectrum.

Following this, we analyzed the transport of the impurity by considering its momentum distribution, showing that the semiclassical picture of an impurity of well-defined quasimomentum emerges after a short time for bosons in the superfluid regime.

ACKNOWLEDGMENTS

T.H.J. thanks Vlatko Vedral for interesting discussions and inviting him to CQT Singapore, where part of this work was completed. T.H.J. and S.R.C. thank John Goold for interesting discussions. M.B. thanks the Swiss National Science Foundation for support through the project PBSKP2/130366. S.R.C. and D.J. thank the National Research Foundation and the Ministry of Education of Singapore for support.

APPENDIX: TIME-EVOLVING BLOCK DECIMATION

The TEBD algorithm efficiently simulates both the unitary and imaginary time evolution (according to $e^{-i\hat{H}t}$ and $e^{-\hat{H}t}$, respectively) of quantum systems comprising a one-dimensional lattice of subsystems, each with a finite number of configurations, where $\hat{H}$ is composed of nearest-neighbor terms [14,15]. It does this by storing the state of a system as a matrix product state (MPS) of dimension χ. In general, for an exact representation of the state vector, the dimension χ and hence the resources required for the simulation must grow exponentially with the size of the lattice. However, for ground and low-lying excited states of one-dimensional systems, near-exact accuracy can be obtained using a much smaller χ that does not grow exponentially with system size [51,52]. With this being the case and using a Suzuki-Trotter decomposition of the operator $e^{-i\hat{H}\delta t}$ (without the i for imaginary time evolution) [53], the evolution may be simulated by the application of a polynomial number of two-site gates, each followed by a recompression into MPS form, which can be done efficiently. For details, we refer the reader to [14,15,54,55].

Our system, described in Sec. II, is of this type, provided we restrict the occupancy of the bosonic lattice to a finite number. To realize our scheme, we first used TEBD to find the ground state of the bosonic part of the system, with an on-site potential U_{ab} added at each site corresponding to an impurity. The initial state of the whole system was then the tensor product of this bosonic state with the initial state of the impurity, which consists of Fock states with occupancies 0 or 1. Next, TEBD was used to simulate the evolution of this state under the full Hamiltonian $\hat{H} = \hat{H}_a + \hat{H}_b + \hat{H}_{ab}$. Expectation values, such as bosonic and impurity densities, were easily extracted from the numerics due to the efficient contractibility of an MPS.

For our simulations, we used a maximum boson lattice-site occupancy of 4 and the largest MPS dimension we used was $\chi = 120$. Our time step was $\delta t = 5 \times 10^{-3}\hbar/J_b$. These parameters were sufficient for the time-evolution considered here; we found that increasing χ and decreasing δt resulted in no significant changes to the observables computed.

[1] M. Lewenstein, A. Sanpera, V. Ahufinger, B. Damski, A. Sen, and U. Sen, Adv. Phys. **56**, 2 (2007).
[2] I. Bloch, J. Dalibard, and W. Zwerger, Rev. Mod. Phys. **80**, 885 (2008).
[3] G. E. Astrakharchik and L. P. Pitaevskii, Phys. Rev. A **70**, 013608 (2004).
[4] A. V. Ponomarev, J. Madroñero, A. R. Kolovsky, and A. Buchleitner, Phys. Rev. Lett. **96**, 050404 (2006).
[5] A. Klein, M. Bruderer, S. R. Clark, and D. Jaksch, New J. Phys. **9**, 411 (2007).
[6] M. Bruderer, A. Klein, S. R. Clark, and D. Jaksch, New J. Phys. **10**, 033015 (2008).
[7] J. Tempere, W. Casteels, M. K. Oberthaler, S. Knoop, E. Timmermans, and J. T. Devreese, Phys. Rev. B **80**, 184504 (2009).
[8] M. Bruderer, T. H. Johnson, S. R. Clark, D. Jaksch, A. Posazhennikova, and W. Belzig, Phys. Rev. A **82**, 043617 (2010).
[9] A. Privitera and W. Hofstetter, Phys. Rev. A **82**, 063614 (2010).
[10] M. A. Cazalilla, Phys. Rev. A **67**, 053606 (2003).
[11] J. Catani, G. Lamporesi, D. Naik, M. Gring, M. Inguscio, F. Minardi, A. Kantian, and T. Giamarchi, e-print arXiv:1106.0828v1 [cond-mat.quant-gas] (2011).
[12] S. Palzer, C. Zipkes, C. Sias, and M. Köhl, Phys. Rev. Lett. **103**, 150601 (2009).
[13] L. Rutherford, J. Goold, Th. Busch, and J. F. McCann, Phys. Rev. A **83**, 055601 (2011).
[14] G. Vidal, Phys. Rev. Lett. **91**, 147902 (2003).
[15] G. Vidal, Phys. Rev. Lett. **93**, 040502 (2004).
[16] J. Stenger, S. Inouye, A. P. Chikkatur, D. M. Stamper-Kurn, D. E. Pritchard, and W. Ketterle, Phys. Rev. Lett. **82**, 4569 (1999).
[17] T. Stöferle, H. Moritz, C. Schori, M. Köhl, and T. Esslinger, Phys. Rev. Lett. **92**, 130403 (2004).
[18] E. Haller, R. Hart, M. J. Mark, J. G. Danzl, L. Reichsöllner, M. Gustavsson, M. Dalmonte, G. Pupillo, and H.-C. Nägerl, Nature (London) **436**, 597 (2010).
[19] C. Kollath, A. Iucci, T. Giamarchi, W. Hofstetter, and U. Schollwöck, Phys. Rev. Lett. **97**, 050402 (2006).
[20] S. R. Clark and D. Jaksch, New J. Phys. **8**, 160 (2006).
[21] M. Greiner, O. Mandel, T. Esslinger, T. W. Hänsch, and I. Bloch, Nature (London) **415**, 39 (2002).

[22] B. Gadway, D. Pertot, J. Reeves, and D. Scheble, e-print arXiv:1104.2564v1 [cond-mat.quant-gas] (2011).
[23] C. Weber, S. John, N. Spethmann, D. Meschede, and A. Widera, Phys. Rev. A **82**, 042722 (2010).
[24] S. Will, Th. Best, S. Braun, U. Schneider, and I. Bloch, Phys. Rev. Lett. **106**, 115305 (2011).
[25] K. W. Madison, C. F. Bharucha, P. R. Morrow, S. R. Wilkinson, Q. Niu, B. Sundaram, and M. G. Raizen, Appl. Phys. B **65**, 693 (1997).
[26] G. H. Wannier, Phys. Rev. **52**, 191 (1937).
[27] N. W. Ashcroft and N. D. Mermin, *Solid State Physics*, 1st ed. (Harcourt College Publishers, Orlando, 1976).
[28] F. Rossi, in *Theory of Transport Properties of Semiconductor Nanostructures*, edited by E. Schöll (Chapman and Hall, London, 1998), p. 288.
[29] Q. Thomen, J. C. Garreau, and V. Zehnlé, J. Opt. B **6**, 301 (2004).
[30] K. Leo, *High-Field Transport in Semiconductor Superlattices* (Springer, Berlin, 2003).
[31] L. Esaki and R. Tsu, IBM J. Res. Dev. **14**, 61 (1970).
[32] H. Ott, E. de Mirandes, F. Ferlaino, G. Roati, G. Modugno, and M. Inguscio, Phys. Rev. Lett. **92**, 160601 (2004).
[33] A. Sibille, J. F. Palmier, H. Wang, and F. Mollot, Phys. Rev. Lett. **64**, 52 (1990).
[34] A. V. Ponomarev, Ph.D. thesis, University of Freiburg, 2008).
[35] A. R. Kolovsky, Phys. Rev. A **77**, 063604 (2008).
[36] J. Madroñero, A. V. Ponomarev, A. R. R. Carvalho, S. Wimberger, C. Viviescas, A. Kolovsky, K. Hornberger, P. Schlagheck, A. Krug, and A. Buchleitner, Adv. At. Mol. Opt. Phys. **53**, 33 (2006).
[37] A. Wacker and A.-P. Jauho, Phys. Rev. Lett. **80**, 369 (1998).
[38] V. V. Bryxin and Y. A. Firsov, Solid State Commun. **10**, 471 (1972).
[39] E. Timmermans and R. Côté, Phys. Rev. Lett. **80**, 3419 (1998).
[40] D. Jaksch, C. Bruder, J. I. Cirac, C. W. Gardiner, and P. Zoller, Phys. Rev. Lett. **81**, 3108 (1998).
[41] D. van Oosten, P. van der Straten, and H. T. C. Stoof, Phys. Rev. A **63**, 053601 (2001).
[42] T. D. Kühner, S. R. White, and H. Monien, Phys. Rev. B **61**, 12474 (2000).
[43] C. Kollath, U. Schollwöck, J. von Delft, and W. Zwerger, Phys. Rev. A **69**, 031601(R) (2004).
[44] T. P. Meyrath, F. Schreck, J. L. Hanssen, C.-S. Chuu, and M. G. Raizen, Phys. Rev. A **71**, 041604(R) (2005).
[45] J. Catani, G. Barontini, G. Lamporesi, F. Rabatti, G. Thalhammer, F. Minardi, S. Stringari, and M. Inguscio, Phys. Rev. Lett. **103**, 140401 (2009).
[46] G. Lamporesi, J. Catani, G. Barontini, Y. Nishida, M. Inguscio, and F. Minardi, Phys. Rev. Lett. **104**, 153202 (2010).
[47] A. R. Kolovsky, J. Stat. Mech. (2009) P02018.
[48] W. S. Bakr, J. I. Gillen, A. Peng, S. Fölling, and M. Greiner, Nature (London) **462**, 74 (2009).
[49] J. F. Sherson, C. Weitenberg, M. Endres, M. Cheneau, I. Bloch, and S. Kuhr, Nature (London) **467**, 68 (2010).
[50] A. R. Kolovsky, A. V. Ponomarev, and H. J. Korsch, Phys. Rev. A **66**, 053405 (2002).
[51] F. Verstraete and J. I. Cirac, Phys. Rev. B **73**, 094423 (2006).
[52] J. Eisert, M. Cramer, and M. B. Plenio, Rev. Mod. Phys. **82**, 277 (2010).
[53] M. Suzuki, Phys. Lett. A **146**, 319 (1990); J. Math. Phys. **32**, 400 (1991).
[54] T. H. Johnson, S. R. Clark, and D. Jaksch, Phys. Rev. E **82**, 036702 (2010).
[55] A. J. Daley, C. Kollath, U. Schollwöck, and G. Vidal, J. Stat. Mech. (2004) P04005.